Available online at www.sciencedirect.com
SCIENCE DIRECT®
International Journal of Heat and Mass Transfer 48 (2005) 665–679
International Journal of HEAT and MASS TRANSFER
www.elsevier.com/locate/ijhmt

Non-iterative estimation of heat transfer coefficients using artificial neural network models

S.S. Sablani [a,*], A. Kacimov [b], J. Perret [b], A.S. Mujumdar [c], A. Campo [d]

[a] Department of Food Science and Nutrition, Sultan Qaboos University, P.O. Box-34, Al-Khod PC 123, Muscat, Oman
[b] Department of Soils, Water and Agricultural Engineering, Sultan Qaboos University, P.O. Box-34, Al-Khod PC 123, Muscat, Oman
[c] Department of Mechanical and Production Engineering, National University of Singapore, 10 Kent Ridge Crescent, Singapore
[d] Department of Mechanical Engineering, University of Vermont, Burlington, Vermont, USA

Received 7 June 2003; received in revised form 27 June 2004
Available online 6 November 2004

Abstract

The Inverse Heat Conduction Problem (IHCP) dealing with the estimation of the heat transfer coefficient for a solid/fluid assembly from the knowledge of inside temperature was accomplished using an artificial neural network (ANN). Two cases were considered: (a) a cube with constant thermophysical properties and (b) a semi-infinite plate with temperature dependent thermal conductivity resulting in linear and nonlinear problem, respectively. The Direct Heat Conduction Problems (DHCP) of transient heat conduction in a cube and in a semi-infinite plate with a convective boundary condition were solved. The dimensionless temperature-time history at a known location was then correlated with the corresponding dimensionless heat transfer coefficient/Biot number using appropriate ANN models. Two different models were developed for each case i.e. for a cube and a semi-infinite plate. In the first one, the ANN model was trained to predict Biot number from the slope of the dimensionless temperature ratio versus Fourier number. In the second, an ANN model was developed to predict the dimensionless heat transfer coefficient from non-dimensional temperature. In addition, the training data sets were transformed using a trigonometric function to improve the prediction performance of the ANN model. The developed models may offer significant advantages when dealing with repetitive estimation of heat transfer coefficient. The proposed approach was tested for transient experiments. A 'parameter estimation' approach was used to obtain Biot number from experimental data.

Keywords: Inverse heat conduction problem (IHCP); Back-propagation algorithm; Cube; Semi-infinite plate; Non-linear problem; Sensitivity analysis; Uncertainty analysis

1. Introduction

Direct Heat Conduction Problems (DHCP) are concerned with the estimation of the temperature field inside solid bodies for known initial and boundary conditions, thermophysical properties and heat generation rates. On the other hand, the determination of surface temperatures, heat source rates, and thermophysical properties by utilizing measured temperatures inside solid bodies are classified as Inverse Heat Conduction Problems (IHCP). Such problems are encountered in a multitude of food and process engineering applications. Examples

* Corresponding author. Tel.: +968 515 289; fax: +968 513 418.
E-mail address: shyam@squ.edu.om (S.S. Sablani).

0017-9310/$ - see front matter © 2004 Elsevier Ltd. All rights reserved.
doi:10.1016/j.ijheatmasstransfer.2004.09.005

Nomenclature

A	growth constant (°C/s), nonlinear problem
$2a$	side of cube (m)
B	dimensionless heat transfer coefficient ($=h\sqrt{\alpha_o}/(k_o^2 A)$), nonlinear problem
Bi	Biot number ($h\cdot a/k$)
E	cost function
F	dimensionless time ($=t/t_m$), nonlinear problem
Fo	Fourier number ($\alpha t/a^2$), linear problem
h	heat transfer coefficient (W/m^2 K)
J	sensitivity coefficient
k	thermal conductivity (W/m K)
N	number of measurement
R^2	regression coefficient
x, y z	linear coordinates (m)
X, Y, Z	dimensionless linear coordinates (x/a, y/a, z/a)
s	temperature–time slope, nonlinear problem, ($d\phi/dF$)
S	temperature–time slope, ($d\theta/dFo$)
t	time (s)
T	temperature (K)
$T_f(t)$	variable ambient/fluid temperature (K), nonlinear problem
T_i	initial temperature (K)
T_f	fluid temperature (K)
X	nondimensional coordinate ($=x/(t_m\sqrt{\sigma_o}A)$, nonlinear problem

Greek symbols

α	thermal diffusivity (m^2/s)
σ	standard deviation
θ	dimensionless temperature $(T_f-T)/(T_f-T_i)$, linear problem
ϕ	dimensionless temperature $T/(t_m A)$, nonlinear problem

include sterilization of particulate liquids in continuous systems (aseptic processing), cooling of fresh produce, frying and freezing of food and biological materials. Moreover, the estimation of the heat transfer coefficient also falls under the category of an Inverse Heat Conduction Problem (IHCP). This approach requires experimental measurement of the transient temperatures inside a body of known geometry at a specified location, usually at the center, and estimation of transient temperatures, at the same location, by solving the governing heat conduction equations with an assumed convective boundary condition (i.e., the Biot number, *Bi*). In doing so, *Bi* is varied systematically to produce computed temperature-time histories closely matching to the experimentally measured temperature histories. The procedure involved is iterative in nature and needs a long computation time. Although this approach for estimating *Bi* is more computationally intensive than conventional approaches, it may have an advantage in a simpler setup and less expensive equipment [1]. Several algorithms based on finite difference and finite element methods have been developed for solving the IHCP. Excellent discussion of the difficulties encountered in solving the IHCP and several solution methods used can be found in Beck et al. [2], Beck and Arnold [3], Alifanov [4] and Ozisik and Orlande [5].

The need for accuracy, fast response and non-iterative solutions to many physical problems has led to the widespread application of artificial neural networks (ANN)[6–15]. ANN is a potent computer model that learns from examples through iterations without requiring prior knowledge of the relationships of the process parameters. ANN is also capable of dealing with uncertainties, noisy data, and nonlinear relationships [14,15]. The salient feature of ANNs that make them attractive for many different applications is their ability to learn and generalize the relationship in complex data sets.

The objective of the present study was to devise a single and direct procedure for estimating the heat transfer coefficient from a numerically/analytically generated temperature field in a cube and semi-infinite plate using ANN to avoid the use of a time-consuming, iterative solution. The problem considered in this work has relevance in food processing operations such as transient heat transfer analysis during drying, frying and freezing of small fruit and vegetable cubes, and sterilization of particulate liquids in continuous systems (aseptic processing). All of these require knowledge of heat transfer coefficients.

2. Formulation

2.1. Linear problem

2.1.1. The direct heat conduction problem (DHCP)

Consider the problem of transient heat conduction in an isotropic cube exposed to a forced flow of a viscous fluid. The thermophysical properties of the fluid and solid, as well as the heat transfer coefficient at all faces of the cube were assumed to be constant. The governing

tri-dimensional heat conduction equation in non-dimensional form is:

$$\frac{\partial^2\theta}{\partial X^2}+\frac{\partial^2\theta}{\partial Y^2}+\frac{\partial^2\theta}{\partial Z^2}=\frac{\partial\theta}{\partial Fo} \tag{1}$$

The initial and boundary conditions that are imposed in Eq. (1) are:

$$\text{For}\quad Fo=0\quad \theta=1\quad \text{for all } X, Y \text{ and } Z \tag{2a}$$

$$\frac{\partial\theta}{\partial X}=0 \text{ at } X=0\quad \text{for all } Y \text{ and } Z,\quad Fo\geqslant 0 \tag{2b}$$

$$\frac{\partial\theta}{\partial Y}=0 \text{ at } Y=0\quad \text{for all } X \text{ and } Z,\quad Fo\geqslant 0 \tag{2c}$$

$$\frac{\partial\theta}{\partial Z}=0 \text{ at } Z=0\quad \text{for all } X \text{ and } Y,\quad Fo\geqslant 0 \tag{2d}$$

$$\frac{\partial\theta}{\partial X}=-Bi\ \theta \text{ at } X=1\quad \text{for all } Y \text{ and } Z,\quad Fo>0 \tag{2e}$$

$$\frac{\partial\theta}{\partial Y}=-Bi\ \theta \text{ at } Y=1\quad \text{for all } X \text{ and } Z,\quad Fo_o>0 \tag{2f}$$

$$\frac{\partial\theta}{\partial Z}=-Bi\ \theta \text{ at } Z=1\quad \text{for all } X \text{ and } Y,\quad Fo>0 \tag{2g}$$

where θ is the non-dimensional temperature, X, Y, and Z are the non-dimensional coordinates, Fo is the Fourier number or dimensionless time and Bi is the Biot number. The finite element based computer software FIDAP (Fluent Inc., NH) was used to solve this conduction problem with a convective boundary condition. A grid refinement study was made to determine the sensitivity of the results to the number of grid points. The final results were generated using a uniform grid with 11 nodal points in each coordinate direction, since no significant differences in the center point temperature response were noted beyond this level. $\Delta\ Fo$ was selected between 0.002 and 0.05 depending upon the value of Bi. The Biot number varied from 0.01 to 10. The increment of Bi increased with increasing Bi. The FIDAP program was run for 65 values of Bi thus obtaining the temperature history at several locations ($X=0$, 0.2, 0.4, 0.6 and 0.8 with Y and $Z=0$). Since the non-dimensional center temperature varied linearly with Fourier number when plotted on a semi-log scale, the temperature profile could be characterized using the slope, S, of this curve. The slope was obtained from calculated temperature histories at five locations for the 65 Bi values. Thus 325 cases were used in the development of the ANN models. The Biot number and the corresponding slope data set of 325 cases was divided into two groups. The first group consisted of 245 cases for training/testing of ANN models while the second group had 80 cases for validation of the ANN model, chosen randomly from the set of 325 cases.

2.1.2. Analytical solution

Carslaw and Jaeger [16] (pp. 184–186) reported a rigorous solution (obtained by separation of variables) to the boundary value problem Eq. (1–2) for an arbitrary rectangular parallelepiped. For a specific case of a cube this solution at the center point yields:

$$\theta(0,0,0,Fo)=8Bi^3\left[\sum_{n=1}^{\infty}\frac{\exp(-A_n^2Fo)}{(Bi^2+Bi+A_n^2)\cos A_n}\right]^3 \tag{3}$$

where A_n are solutions of the equations $A_n\tan A_n = Bi$. Modern computer algebra (Wolfram [17]) allowed us to reproduce all standard thermal characteristics (in particular, temperature contour plots in specified parallelepiped cross-sections, flux vector field and volume averaged temperature). We notice that the roots A_n of our nonlinear equation as well as of all equations listed in Appendix IV of Carslaw and Jaeger [16] are readily found as **FindRoot** *Mathematica* routine. The results obtained by FiDAP are in excellent agreement with those computed analytically. For instance, the analytical slopes for $Bi=0.01$, 0.1, 1, 10 are $S=-0.012985$, -0.12606, -0.96436, -2.6601 whilst ANN gives -0.01297, -0.12575, -0.95734, -2.61915. We used the same built-in option of *Mathematica* to solve the inverse problem requiring determination of the roots of $Bi=f(\theta, Fo)$ from the series equation above. For this case, with one nonlinear equation involving an infinite number of other nonlinear equations the solution is not so straightforward.

Similarly, we can easily handle other geometries, inhomogeneous boundary conditions (in particular, spatially non-uniform Bi and heat generation terms), if the variables in Eq. (1) separate or integral Green function representations are available (e.g., Malov et al [18]; Yen et al. [19]) because *Mathematica* with minimal programming efforts treats nonlinear equations, double-triple series and integrals. However, the analytical approach, if one taps all its exactitude (in our case it implied sensitivity to the number of terms retained in the series and *post-audit* of the uniqueness of the roots found), calls for a meticulous analysis and availability of computer algebra packages that might be not possible in practical situations.

2.2. Non-linear problem

Consider the problem of transient heat conduction in a semi-infinite plate exposed to a forced flow of a viscous fluid. It is assumed that the material is homogeneous but its thermal conductivity is a function of temperature:

$$k=k_oT^n \tag{4}$$

where k_o and n are two arbitrary positive constants. Without any loss of generality (see other finite-support solutions in Samarskii et al., [20]) we assume that

$n = 1$. We also assume that both the solid and ambient fluid are at zero temperature at $t < 0$ and at $t = 0$ the ambient temperature starts rising as:

$$T_f = At \quad 0 < t < \infty \tag{5}$$

where A (°C/s) is the growth constant. As above, we assume that at the interface between the body and fluid ($x = 0$) the third-type boundary condition holds:

$$T\frac{dT}{dx} = h/k_o(T - T_f) \tag{6}$$

We assume that the density ρ and heat capacity C_p of the medium are constant. Then the governing equation for 1-D conduction is:

$$\alpha_o \frac{\partial}{\partial x}\left(T\frac{\partial T}{\partial x}\right) = \frac{\partial T}{\partial t}, \tag{7}$$

where

$$0 \leqslant x \leqslant \infty, \quad 0 \leqslant t \leqslant \infty.$$

In Eq. (7) $\alpha_o = k_o/(\rho C_p)$ is the benchmark thermal diffusivity. Although it is constant, the thermal diffusivity itself is not owing to variations in conductivity. The temperature T_m at a certain instant t_m and certain point x inside the body can be estimated. By introducing the following dimensionless quantities:

$$\phi = T/(t_m A), F = t/t_m, X = x/(t_m\sqrt{\alpha_o A}),$$
$$B = h\sqrt{\alpha_o/(k_o^2 A)} \tag{8}$$

the boundary-value problem Eqs. (5)–(7) can be re-written as:

$$\phi_f = F \quad 0 < F < \infty \tag{9}$$

$$\phi\frac{d\phi}{dx} = B(\phi - F) \quad \text{at } x = 0 \tag{10}$$

$$\frac{\partial}{\partial X}\left(\phi\frac{\partial\phi}{\partial X}\right) = \frac{\partial\phi}{\partial F} \tag{11}$$

2.2.1. Analytical solution

Barenblatt's [21] traveling wave solution to Eq. (11) is:

$$\phi = sX + s^2F \quad \text{at} \quad X < X_0 \tag{12}$$

$$\phi = 0 \quad \text{at} \quad X > X_0 \tag{13}$$

where $X_0(t) = -s^*F$ is a dimensionless depth of the propagation of the heat front into the body. As it is clear from Eq. (12), to measure temperature at any X one should wait until the front crosses this point. We recall that in linear problems the reaction to any change of the ambient temperature spreads instantaneously over the whole solid body that is mathematically called an "infinite speed" (celerity).

In order to calculate the constant s we put Eq. (12) into Eq. (10) and arrive at a cubic equation:

$$s^3 - Bs^2 + B = 0 \tag{14}$$

Since the Barenblatt solution must have a finite speed of propagation of the thermal wave from the three roots of Eq. (14), we need only a real and negative (a positive root gives a solution of Eq. (7) which does not satisfy the initial condition). The negative root is found by the Cardano formula as:

$$s = B/3 - \frac{(1 + I\sqrt{3})B^2}{3^*2^{2/3}(2B^3 - 27B + 3B\sqrt{81 - 12B^2})^{1/3}} - \frac{(1 - I\sqrt{3})(2B^3 - 27B + 3B\sqrt{81 - 12B^2})^{1/3}}{6^*2^{1/3}} \tag{15}$$

where I is an imaginary unit. We note that instead of the ambient regime (Eq. (5)) and nonlinearity (Eq. (4)) other functions leading to explicit solutions from Barenblatt et al. [21] can be used for matching the third-type boundary condition at $x = 0$ (of special interest are the blow-up solutions). Some properties of these solutions (e.g. comparison theorems, Samarskii et al., [20]) are intuitively clear and do not differ qualitatively from the linear conduction case. However, the solutions for several other temperature functions when applied at the boundary are surprising and not obvious. For example, the case of rapid temperature rise at the boundary results is localization of temperature front; this is not encountered in linear heat conduction problems.

2.2.2. Training of the artificial neural network model

The feed forward network structure [22] was used in this study. The structure of network with transfer function and computation equation for neurons of different layers is shown in Fig. 1. Several ANN models were trained and tested using the training data set. In the case of a cube, for the inverse problem, the input layer consisted of two neurons corresponding to each of the input parameter (slope, S, and location, X) while the output layer had one neuron representing the Biot number, Bi. In developing the ANN model for the direct problem, Bi and S were switched. In the case of the semi-infinite plate, the input and output layers consisted of one neuron in each layer. The number of hidden layers and the neurons within each hidden layer can be varied based on the complexity of the problem and the data set. In order to reduce the chances of memorization of the behavior within the data set (rather than generalization), the number of hidden layers and neurons in these layers ought to be minimized [13]. In our study, only one hidden layer was chosen while the neurons in that layer were varied from 1 to 10, in increments of one. This resulted in a total of 10 networks. The optimal configuration was based upon minimizing the difference between the ANN predicted values and the desired outputs.

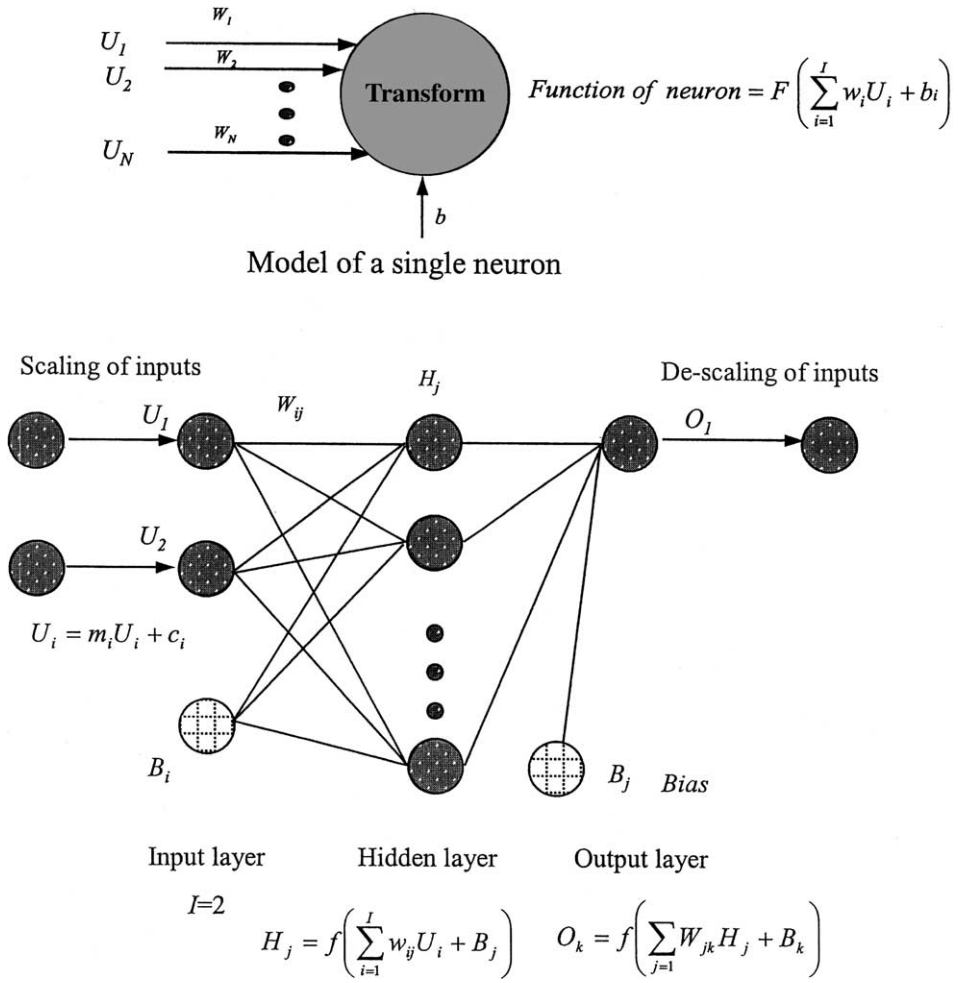

Fig. 1. A schematic diagram of a single neuron, and multi-layer artificial neural network used for the inverse and direct heat conduction problem.

The commercial software package, Neural Works Professional II/Plus (Neural Ware, Pittsburgh, PA), was employed in the study. The back-propagation algorithm was utilized for model training. In order to train a model, several parameters including the learning rule, the transfer function, the learning coefficient ratio, the random number seed, the error minimization algorithm, and the number of learning cycles, need to be specified. These parameters could be varied based on the complexity of the problem. Given the lack of clear guidance in the literature concerning the selection of the above parameters, a trial-and-error procedure must be followed. While some of the parameters were kept constant during our study, others were varied to develop the optimum ANN configuration. The parameters that were kept constant include the transfer function (the hyperbolic-tangent transfer function); the learning rule (the normalized-cumulative delta-rule), the random number seed (257), and the learning rate (0.9), momentum (0.6). The error-minimization process was achieved using the gradient descent rule [22] while the number of training cycles was set at 200 000. All of the remaining model parameters (as specified above) were kept constant throughout the training processes.

The back-propagation scheme uses the supervised training technique where the network weights and biases are initialized randomly at the beginning of the training phase. For a given set of inputs to the network, the response to each neuron in the output layer is calculated and compared with the corresponding desired output response. The errors associated with the desired output response are adjusted in such a way that it reduces these errors in each neuron from the output to the input layers. To avoid the potential problem of over-training or memorization while employing the back-propagation algorithm, the option of saving the best configuration

was selected in order to only save the network with the best result during the large number (~200 000) of training cycles.

2.2.3. Selection of the optimal ANN configuration

The performance of various ANN configurations was compared using the mean relative error (MRE) and the standard deviations in the relative (STD_R) errors. The coefficient of determination, R^2, of the linear regression line between the predicted values from the neural network model and the desired output was also used as a measure of performance. The three error measuring parameters used to compare the performance of the various ANN configurations were [13,15,23]:

$$BIAS = \frac{1}{N}\sum_{i=1}^{N}\Delta B_R \tag{16}$$

$$MRE = \frac{1}{N}\sum_{i=1}^{N}ABS(\Delta B_R) \tag{17}$$

$$STD_R = \sqrt{\frac{\sum_{i=1}^{N}(\Delta B_R - \overline{\Delta B_R})^2}{N-1}} \tag{18}$$

where $B_R = (B_P - B_D)/B_D$. The parameter B_P represents the predicted output from the neural network model for a given input while B_D is the desired output (i.e. exact data) from the same input that was produced by DHCP.

The coefficient of determination, R^2, of the linear regression line between the predicted values from the neural network model and the desired output was also used as a measure of performance.

2.2.4. The iterative "parameter estimation" approach

The transient temperatures at the center of the cube with known physical and thermal properties were estimated by solving the governing heat conduction Eqs. (1–2) with an assumed Biot number/convective heat transfer coefficient using the FIDAP program. The Biot number/heat transfer coefficient was then varied to produce several time-temperature profiles and the slopes were computed from these temperature profiles. The *Bi* for transient temperatures obtained from experiment was then estimated by minimizing the following function, called the cost function:

$$E = \sum_{i=1}^{N}[S_{exp} - S_{num,i}]^2 \tag{19}$$

The slope, S_{exp} was obtained from the experimental time-temperature data as described in the previous section. The transient temperatures at the center of the cube were obtained for a range of *Bi*. Using transient temperature data values of $S_{num,i}$ were computed. The cost function E was determined using Eq. (19) for various *Bi* values and at the minimum value of E, corresponding *Bi* was taken as experimental *Bi*. In this iterative procedure, the Biot number was refined and the stopping criteria used was set as $E \leqslant 10^{-6}$ at lower range ($1 < Bi < 1.6$) and $E \leqslant 10^{-4}$ at higher range ($5 < Bi < 8$) of Biot number. In last equation minimizing E with respect to parameters *Bi* leads to:

$$\frac{\partial E}{\partial Bi} = 0 \Rightarrow \sum_{i=1}^{M}\frac{\partial S_{num,i}}{\partial Bi_i}(S_{exp} - S_{num,i}) \tag{20}$$

Sensitivity coefficient (J_i) was then obtained with respect to *Bi*

$$J_i = \frac{\partial S_{num,i}}{\partial Bi_i} \tag{21}$$

2.2.5. Statistical considerations in parameter estimation

Experimental measurements of temperatures are not exact. Measurement errors in temperature produce error in the estimation of slope that may be amplified by the ill-posed character of the inverse problem. One way to verify the robustness of the inverse problem algorithm is to introduce Gaussian noise with an average zero mean and a constant variance σ^2 (or standard deviation, σ) to the measured temperature [3,24]. The statistical properties of the estimated parameters with and without noise are then correlated. The confidence limits in the estimated parameters (i.e. *Bi*) with a confidence interval at 99% were estimated as $\pm 2.576 \times \sigma$ [3,24].

3. Results and discussion

3.1. Linear problem

Two forms of the training data set were prepared, namely, (1) *Bi* as dependent (output parameter), and *S* and *X* as independent (input) variables, in the case of the inverse problem and, (2) *S* as dependent and *Bi* and *X* as independent (input) variables, in the case of the direct problem. In each case, a data set of 245 conditions was used for training the ANN models. Different ANN configurations were trained using the original as well as the transformed variables. In each analysis, the ANN configuration (out of 10) that minimized the four error measuring parameters and optimized R^2 was ultimately selected as the optimum.

3.1.1. The inverse heat conduction problem

In the first attempt, the ANN models were trained using an original data set without applying any transformation to the Biot number or to the slope *S*. The configuration of the ANN model was varied, as discussed above. However, the performance of many ANN config-

Table 1
Associated prediction errors of the Biot number, *Bi*, for cube/fluid assembly with different ANN configurations before transformations of data

# of Neurons in hidden layer	BIAS (%)	MRE (%)	STD_R (%)	R^2
1	−127	145	374	0.988
2	−6.16	12.6	33.7	0.999
3	−0.247	16.3	44.5	0.999
4	−5.77	14.4	39.3	0.999
5	−14.3	15.0	41.7	0.999
6	−15.4	15.9	44.5	0.999
7	−6.22	10.0	31.5	0.999
8	−2.63	9.88	23.3	0.999
9	−8.69	11.6	37.0	0.999
10	−42.9	43.1	97.9	0.999

urations was not very satisfactory (Table 1), since the MRE and STD_R in the prediction of *Bi* always exceeded 9% and 23, respectively. This was particularly true for the prediction *Bi* in the lower range ($Bi = 0.01$ to 1.0). An attempt was made to improve the results by changing some of the neural network parameters such as transfer functions and learning rate. However, this approach did not improve the predictive performance of the ANN models.

In principle, ANN models do not require any prior knowledge of the relationships between dependent and independent variables. However, in some problems, transformation of the independent or/and dependent variables is known to improve their predictive performance [9,13]. For examples, friction factor in pipe flow problems was correlated with Reynolds number on logarithmic scale [13], heat transfer coefficient in tubes was correlated with thermal, physical and flow properties in terms of dimensionless numbers such as Nusselt, Reynolds, Prandtl and Eckert numbers [23]. A plot of *Bi* versus *S* indicated that arctangent relationship between *Bi* and *S* as shown in Fig. 2 [25]. Analytical solution of system of Eqs. (1–2) also showed tangent relationship between *Bi* and one of the parameter in Eq. (3). Hence, both *Bi* and *S* were transformed using the inverse tangent functions $\tan^{-1} Bi$ and $\tan^{-1} S$ before feeding to the ANN model. This transformation led to a significant improvement in the prediction performance of all ANN models (Table 2). The optimal ANN configuration included five neurons in the hidden layer. The MRE for this optimal configuration was 1.8%, with a standard deviation of 3.3%. Other trigonometric functions such as exponential transformation were also used but they did not improve the prediction performance. The prediction error (i.e. relative error) of optimal network in the higher range of *Bi* ($7.0 < Bi < 10.0$) was between 4 and 7%. This is why the standard deviation in relative error was slightly higher than mean relative error. Fig. 3 shows a plot of the predicted versus desired values of *Bi* using the optimal neural network.

Two of the simplest ANN models with three neurons and four neurons also predicted *Bi* with very good accuracy (MRE < 2.5%). Considering the benefits of a non-iterative procedure, an ANN model with three hidden neurons can be considered a very good predictor. This particular model shows excellent accuracy (MRE of 1.4%) for the prediction of *Bi* in the range of *Bi* between 0.04 and 10.0. This model is recommended to users. The network weights and coefficients associated with this ANN model are presented in Table 8 Appendix A.

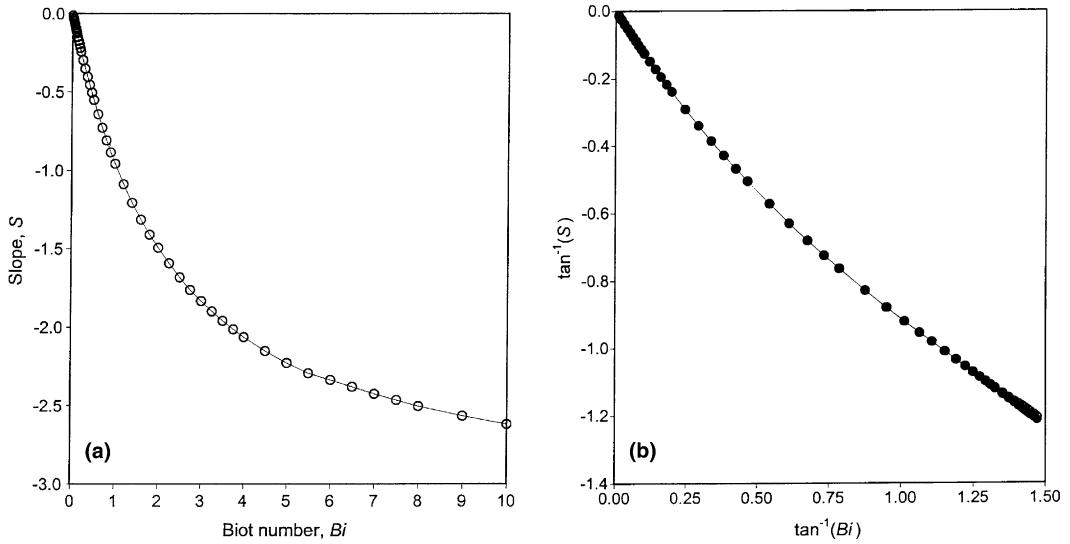

Fig. 2. Relationship between slope and Biot number.

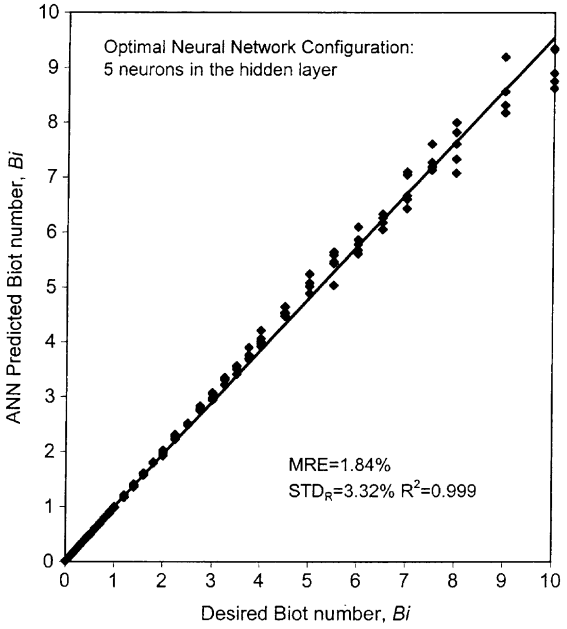

Fig. 3. Predicted versus desired values of the Biot number.

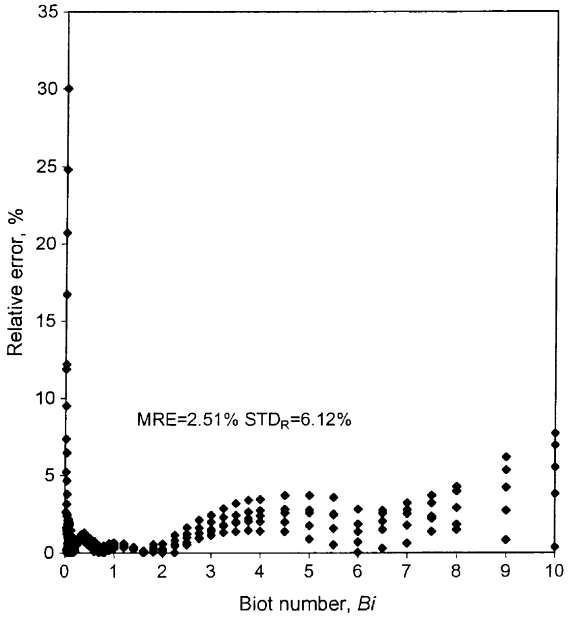

Fig. 4. Relative errors in the prediction of Biot number using simple ANN configuration with two neurons in the hidden layer.

These equations can be used to predict *Bi* from the slope of experimental measured transient temperatures at any location ($0 \leqslant X \leqslant 0.8$) within the cube. The associated relative errors with the prediction of *Bi* using network weights and coefficient presented in the Table 8 are shown in Fig. 4.

3.1.2. The direct heat conduction problem

Determination of the transient temperatures at the center of the cube for a given *Bi* does not involve iterative solution. Numerical methods can easily be employed for this purpose. However, this does involve writing a computer code or the use of commercial software. The data set consisting of *Bi* and the corresponding *S* used in the previous section was also used to correlate them in a direct manner (i.e. *Bi* and *X* as inputs and *S* as output parameter). The original as well as transformed (using arctangent function) data sets were used to train different ANN configurations. The errors associated with these configurations are summarized in Tables 3 and 4. Once again, the transformed data improved the predictive performance of ANN model significantly. In this case, one of the simplest ANN model with two hidden neurons was also the optimal configuration. The MRE for this optimal configuration was 2.5%, with a standard deviation of 8.2%. The network weights and coefficients associated with this simple ANN model are presented in Table 9 Appendix A. These equations can be used to predict *S* at the center of cube (hence transient temperatures) for a given Biot number.

Table 2
Associated prediction errors of the Biot number, *Bi*, for cube/fluid assembly with different ANN configurations after transformations of data

# of Neurons in hidden layer	BIAS (%)	MRE (%)	STD$_R$ (%)	R^2
1	4.09	18.0	29.1	0.971
2	−7.68	18.5	44.2	0.979
3	−1.63	2.51	6.12	0.999
4	−0.181	2.02	4.05	0.998
5	−0.829	1.84	3.32	0.998
6	−1.28	2.21	5.12	0.999
7	−0.458	1.96	4.10	0.999
8	−1.34	2.17	5.13	0.999
9	−0.569	1.99	4.51	0.999
10	1.52	1.98	2.30	0.998

3.1.3. Verification of the ANN models

The predictive performance of both ANN models (one for inverse and another for direct problem) was validated using a data set of 80 cases, which were not used in the initial training of the ANN models. In the case of the inverse problem, the simple ANN model (2 hidden neurons) predicted *Bi* with a mean relative error of 2.3%, a standard deviation in relative error of 5.5%, and a coefficient of determination of 0.9994. For the direct problem, ANN model with two hidden neurons predicted *S* with a mean relative error of 2.2%, a standard deviation of relative error of 5.6%, and a coefficient

Table 3
Associated prediction errors of the slope, S, for cube/fluid assembly with different ANN configurations before transformations of data

# of Neurons in hidden layer	BIAS (%)	MRE (%)	STD_R (%)	R^2
1	−80.1	81.5	213	0.991
2	−8.25	10.8	32.4	0.997
3	−5.34	8.71	25.3	1.000
4	−6.43	9.39	27.8	1.000
5	−8.13	10.4	31.3	1.000
6	−9.63	11.5	34.9	1.000
7	−11.2	12.7	38.4	1.000
8	−2.63	7.35	19.6	1.000
9	−22.1	23.4	72.3	1.000
10	−8.26	11.3	34.2	1.000

Table 4
Associated prediction errors of the slope, S, for cube/fluid assembly with different ANN configurations after transformations of data

# of Neurons in hidden layer	BIAS (%)	MRE (%)	STD_R (%)	R^2
1	−5.33	14.2	30.5	0.992
2	−1.43	2.52	8.15	1.000
3	−2.74	3.18	10.6	1.000
4	−2.12	2.78	8.90	1.000
5	−0.716	2.03	5.78	1.000
6	−0.895	2.15	6.39	1.000
7	−1.519	2.40	7.46	1.000
8	−1.055	3.46	11.1	1.000
9	−0.235	1.92	5.01	1.000
10	−1.62	2.37	7.71	1.000

of determination of 1.000. Once again the standard deviations are higher than the mean relative errors since the errors in predictive performance for Bi less than 0.04 were rather high (~20%). Otherwise, the mean relative errors in prediction of Bi and S using ANN models were less than 1% in the Biot number range between 0.04 and 10.0.

3.2. Non-linear problem

ANN models for semi-infinite plate were developed using the data that were transformed using arctangent functions. The training data consisted of 100 cases non-dimensional heat transfer coefficient, B and slope (of dimensionless temperature ϕ and dimensionless time F) s, at know location $X = 0.2$ as variables. A data set of 100 conditions was used for training the ANN models. The optimal ANN configuration included seven neurons in the hidden layer. The MRE for this optimal configuration was less than 1.0%, with a standard deviation of 2.9%. The accuracy of simplest model i.e. one or two neuron(s) in the hidden layer for was also very good (MRE < 2%, see Table 5). This demonstrated the capability of neural network to generalize the behavior of the nonlinear problems. Islam et al. [26] also developed the neural network with four inputs (i.e. temperature, velocity and humidity of air, and product thickness) and two outputs (drying rate parameters) to predict the drying behavior of potato slices. They solved a highly nonlinear problem of simultaneous heat and mass diffusion in thin potato slices with temperature and moisture dependent thermal conductivity, density and moisture diffusivity to generate data for training their ANN model using back-propagation algorithm. The mathematical model also included temperature dependent thermodynamic properties of air/water system. The trained network was then validated using randomly generated test cases as input. They showed that ANN was able to make excellent predictions for the multi-dimensional data.

Table 5
Associated prediction errors in the dimensionless heat transfer coefficient, B, for nonlinear problem with different ANN configurations after transformations of data

# of Neurons in hidden layer	BIAS (%)	MRE (%)	STD_R (%)	R^2
1	1.094	1.96	6.57	1.000
2	1.206	2.34	7.01	1.000
3	0.233	3.32	8.28	0.999
4	−1.047	2.56	5.04	0.999
5	0.197	1.70	4.41	1.000
6	1.459	2.39	4.89	0.999
7	0.576	0.92	2.86	1.000
8	0.748	1.16	3.88	1.000
9	0.630	1.15	3.46	1.000
10	0.357	1.21	4.47	1.000

The predictive performance of ANN models (optimal with seven neurons and the simplest with one neuron in hidden layer) was validated using a data set of 22 cases, which were not used in the initial training of the ANN models. The optimal and the simple ANN model (two hidden neurons) predicted B with a mean relative error of 1.0 and 0.6%, respectively. The network weights and coefficients associated with the simplest ANN model (i.e. a single neuron) are presented in Table 10 Appendix A.

The non-linear problem presented here is simple since there is only one input parameter i.e. slope at known location was used. Of course there are most complex problems such as time and temperature dependent heat transfer coefficients could be solved. However there are not so many analytical solutions available to generate the data to train ANN models. In such situations numerical methods alone could be used to generate data. Nevertheless the ANN based approach developed to generate non-iterative solutions described here can be used for more complex problems.

3.2.1. Example of parameter estimation using experimental measurements

Nylon cubes (Hoover Precision Products, Sault Ste Marie, MI) of two different sizes (side = 1.4 and 2.0 cm) and known thermal and physical properties were used for experimental determination of convective heat transfer coefficients in air freezer and convection oven. The density, heat capacity, thermal conductivity and thermal diffusivity of nylon cubes were 1128 kg/m^3, 2073 J/kg K, 0.369 W/m K, 1.51×10^{-7} m^2/s respectively. For the purpose of measuring particle transient temperatures, a fine hole was drilled to the center of the cube, which was filled with a 50%:50% mixture of epoxy resin and hardener, and a fine-wire (0.0762 mm diameter) copper-constantan thermocouple was inserted to the center. In this way, the trapping of air along the channel was minimized. The thermocouple equipped cubes were heated/cooled in convection oven/freezer maintained at constant temperature. Temperatures were recorded at 10 s time intervals using digital thermometer (Omega Engineering Corporation, Stamford, CT).

The heat transfer coefficient/*Bi* values were determined using the iterative procedure of parameter estimation described in previous section. The estimated values of heat transfer coefficients for different conditions are presented in Table 6. The accuracy in estimated and experimental temperature profiles was good and the standard deviation in the temperatures for different experimental condition is given in Table 6. In order to verify the robustness of inverse parameter estimation approach three levels of additional noise (σ = 0.1 °C, 0.5 °C and 5% error in all the measured temperatures) to the transient temperatures was introduced. An example of the errors in the transient temperatures and its results in the estimated parameter *Bi* is presented in Table 7. The results of the 100 parameter estimation with confidence interval are assembled in Fig. 5a and b. At lower range of heat transfer coefficient/*Bi*, there was a relative error of 1.07%, 1.1% and 1.9% for σ = 0.1 °C, 0.5 °C and 5%, respectively. While for higher range of *Bi*, there was a relative error of 0.14%, 0.56% and 1.26 for σ = 0.1 °C, 0.5 °C and 5%, respectively. The results indicated that the *Bi* was less sensitive to introduced errors in transient temperatures obtained at higher range of *Bi*. The sensitivity curve also confirms this trend as shown in Fig. 6. The measured temperatures (or slope) are more sensitive to lower range of *Bi*. As expected results are much more stable for good quality measurements (i.e. σ = 0.1 °C and 0.5 °C) than for poor quality measurements (Fig. 5a and b). These trends are similar for both lower and higher range of *Bi*.

The ANN model developed was also used to estimate convective heat transfer coefficient/Biot number from transient temperatures within the cube obtained from

Table 6
Biot number predicted using ANN model and numerical method (FIDAP) under different experimental conditions

System	Fluid	Side of cube (cm)	Iterative method Numerical method (FIDAP)			ANN Model	
			h (W/m^2 K)	*Bi*	Standard deviation σ, (°C)	h (W/m^2 K)	*Bi*
Freezer	Air, −40 °C	1.4	56.4	1.07	0.427	56.4	1.07
		1.4	57.5	1.09	0.395	57.5	1.09
		2.0	55.5	1.51	0.511	55.6	1.51
		2.0	56.3	1.53	0.501	56.2	1.53
Convection Oven	Air, 70 °C	1.4	278	5.27	0.507	282	5.35
		1.4	282	5.35	0.496	285	5.40
		2.0	271	7.35	0.241	262	7.10
		2.0	274	7.42	0.255	265	7.17

Table 7
Results of an estimation of experimental heat transfer coefficients/Biot number obtained with Gaussian noise of zero mean and different standard deviations

Experimental condition (air temperature and cube size)	*Bi* using parameter estimation approach	Standard deviation (σ) error in all the measured temperature	Mean value of estimated *Bi*	Standard deviation (σ) in estimated *Bi*
−40 °C and 1.4 cm	1.07	0.1 °C	1.059	0.00263
−40 °C and 1.4 cm	1.07	0.5 °C	1.06	0.0125
−40 °C and 1.4 cm	1.07	5%	1.08	0.0415
70 °C and 2.0 cm	7.10	0.1 °C	7.09	0.0424
70 °C and 2.0 cm	7.10	0.5 °C	7.14	0.248
70 °C and 2.0 cm	7.10	5%	7.19	0.941

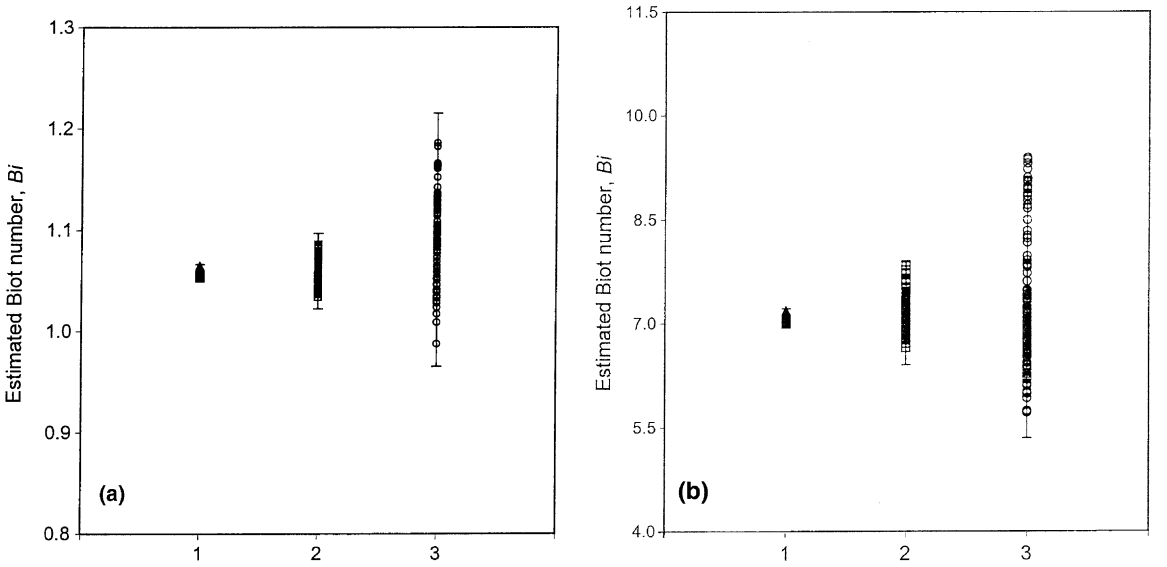

Fig. 5. Biot number estimation results for (a) air temperature −40 °C, cube size 1.4 cm and (b) air temperature 70 °C, cube size 2.0 cm. Results for; (1) $\sigma = 0.1$ °C, (2) $\sigma = 0.5$ °C and (3) $\sigma = 5\%$.

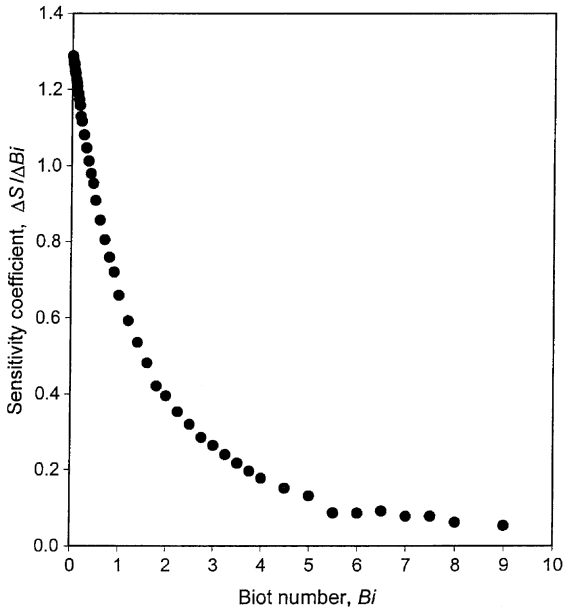

Fig. 6. Sensitivity in slope (temperatures) with respect to Biot number.

experiments. Table 6 shows the values of heat transfer coefficients/Biot numbers predicted using the ANN model and the FIDAP for different experimental conditions. For most cases, the *Bi* predicted was very close to the *Bi* estimated using FIDAP (error <4%). The mean relative error in the ANN-predicted *Bi* was 1.0% and the standard deviation of relative error was 1.0%. This is well below the experimental error (~5–0%) observed in the estimation of the heat transfer coefficients.

3.2.2. Uncertainty analysis

Artificial neural networks are capable of handling uncertainties [13–15,22]. In order to test the generalization capability of artificial neural networks random noise was introduced in the training dataset. The analysis is similar to one used in previous section and also used by Fan et al. [15]. In the case of cube geometry, the Gaussian distribution with zero mean and a standard deviation of 5% in slope was introduced in each input data point (i.e. in slope, *S*). This is the worst-case error in estimated slope. The analysis was also extended to incorporate 5% error in thermocouple location (i.e. *X*). The error distribution is chosen so that with, 99% probability, the error in measured temperature or thermocouple location is less than or equal to the worst-case error. The sensitivity of the optimal network was examined using the full dataset (245 cases) with the noise. A set of 200 different files (i.e. 100 with noise in slope and another 100 with noise in location) with noisy data based on Gaussian distribution was created (with total 49 000 cases). The prediction accuracy of the optimal network with uncertain data was close to that of original data set without noise. The results of the 200 data sets are collected in graphs (Figs. 7 and 8). The prediction accuracy of neural network with noisy data, at higher range of Biot number was in the same range (i.e. 10%) as with observed with original data set. The established neural network has quite a small uncertainty to random

errors in *Bi* less than 8. The Biot number were less sensitive to error in thermocouple location, particularly when used at the center of the geometry, than error in measured temperature (i.e. slope). This demonstrated the capability of ANN in dealing with uncertainties and noise.

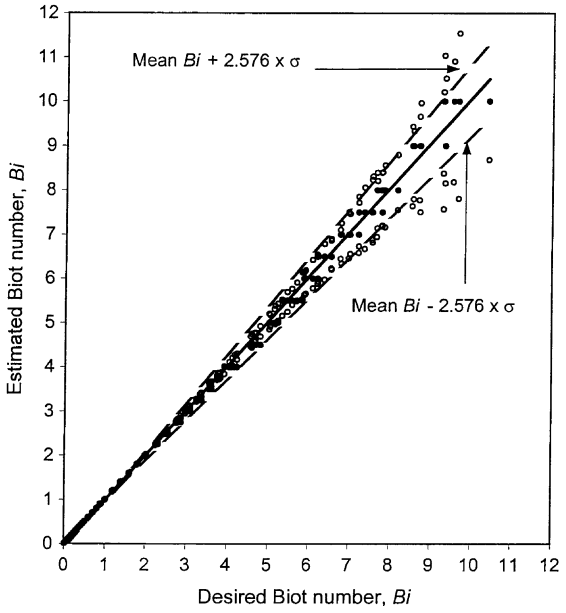

Fig. 7. Biot number estimation results for Gaussian distribution with zero mean and a standard deviation of 5% in slope.

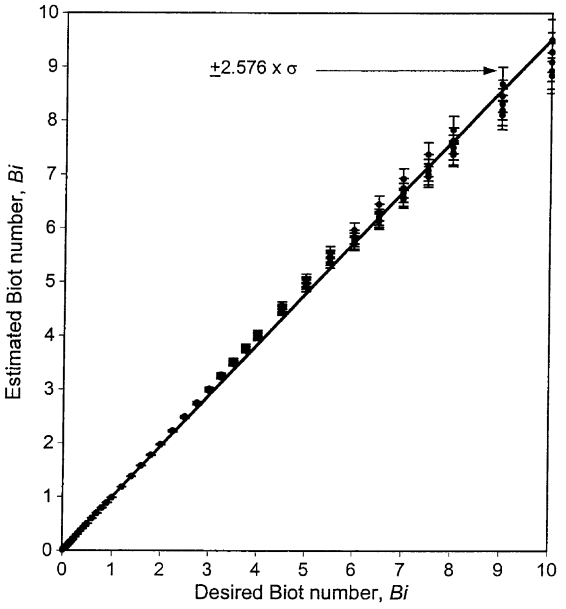

Fig. 8. Biot number estimation results for Gaussian distribution with zero mean and a standard deviation of 5% in thermocouple location.

3.2.3. Sensitivity analysis

The sensitivity of the estimated heat transfer coefficient with respect to assumed values of thermal conductivity and thermal diffusivity was tested by introducing ±5% error in these values. A change in thermal diffusivity alone of a cube by ±5% resulted in a 6.4–7.8% error in the lower range (i.e. in freezer) of h and in its higher range (i.e. in oven) by 14.3–20.6%. The associated errors in calculated h were lower when both thermal diffusivity and thermal conductivity were changed simultaneously. A change of ±5% in thermal diffusivity and conductivity resulted in a 1.8–2.5% and 10–17.4% errors in estimated h in its lower and higher range, respectively. The errors in calculated h were higher under conditions of high Bi/h. This is due to relatively larger internal heat resistance where heat flow was mainly governed by particle thermal diffusivity rather than convective heat transfer. In such situations, metal particle with high thermal conductivity should be chosen over low thermal conductivity particles, in order to reduce the error in estimation of h [27]. The thermocouple misplacement error of 0.7 and 1.0 mm (10% of the half side of cubes) from the center of the particle resulted in overestimation of 0.9–1.5% in calculated heat transfer coefficient/*Bi* values at lower end and at the higher of *Bi*. A further increase in error due to thermocouple misplacement of 20% (1.4 and 2.0 mm), resulted in an overestimation of the heat transfer coefficient by 4.4 to 7.3%. This suggests that, when particle temperatures are measured with thermocouples, the associated error due to thermocouple placement would be lower if the temperatures are measured at the particle center, as opposed to away from center. This is due to associated larger temperature gradients close to the surface, when compared to the gradient at the particle center [27].

4. Conclusions

ANN models are presented to allow prediction of the convective heat transfer coefficient at the surface of a cube and semi-infinite plate from measurement of the temperature-time history inside the solid body. These models are non-iterative, which yield results within 2.5% of those obtained by iterative solution of the governing conduction equation. A simple ANN model for estimation of transient temperatures inside the cube for a range of *Bi* was also presented. Though analytical solutions are available to determine temperature in an arbitrary rectangular parallelepiped as well as in a semi-infinite plate with temperature dependent thermal conductivity subjected to convective heat transfer, estimation of the heat transfer coefficient/*Bi* from known

time temperature data still remains iterative in nature. The neural network models were capable in generalizing the behavior of both linear and nonlinear problems. The ANN models presented here can easily be used without any elaborate programming. The present concept of using neural networks for estimating heat transfer coefficient can easily be extended for complex shapes and temperature dependent boundary conditions. However, as the complexity of the problem increases, different transformation of input/output variables may be required.

Acknowledgments

The authors would also like to thank Dr. Michel Claereboudt of Department of Marine Science and Fisheries, Sultan Qaboos University for his assistance in statistical analysis.

Appendix A

See Tables 8–10.

Table 8
Artificial neural network parameters for estimation of *Bi* from the location and slope of temperature ratio (on logarithm scale) versus *Fo*

i	j	bias	w_{ij}	j	k	bias	w_{jk}
1	1	-5.34×10^{-1}	-2.3×10^{-2}	1	1	4.06×10^{-1}	-7.37×10^{-1}
2	1		6.01×10^{-1}	2	1		1.04×10^{0}
1	2	-1.541×10^{0}	4.26×10^{-3}	3	1		-2.47×10^{-1}
2	2		-1.10×10^{0}				
1	3	-2.27×10^{-1}	6.42×10^{-2}				
2	3		3.14×10^{-1}				

X, $0 \leqslant X < 0.8$
Bi, $0.01 \leqslant Bi \leqslant 10.0$
S, $-2.68 \leqslant S \leqslant -0.013$
Input parameters
U_1X
$U_2 = \text{atan}(S)$
$S_1 = \text{atan}\ (Bi)$
Scaling of input parameters
$m_1 = 2.5\times10^{0}$
$c_1 = -1.0\times10^{0}$
$m_2 = 1.665\times10^{0}$
$c_2 = 1.022\times10^{0}$
De-scaling of output parameter
$m_1 = 1.218\times10^{0}$
$c_1 = 7.41\times10^{-1}$

Table 9
Artificial neural network parameters for estimation of *S* from the location and *Bi*

i	j	bias	w_{ij}	j	k	bias	w_{jk}
1	1	-1.635×10^{0}	-1.124×10^{0}	1	1	6.16×10^{-1}	1.335×10^{0}
2	1		-2.82×10^{-4}	2	1		7.60×10^{-1}
1	2	8.03×10^{-1}	-7.64×10^{-1}				
2	2		-2.36×10^{-3}				

X, $0 \leqslant X \leqslant 0.8$
Bi, $0.01 \leqslant Bi \leqslant 10.0$
S, $-2.68 \leqslant S \leqslant -0.013$
Input and output parameters
$U_1 = \text{atan}(Bi)$
U_2X
$S_1 = \text{atan}\ (S)$
Scaling of input parameters
$m_1 = 1.369\times10^{0}$
$c_1 = -1.014\times10^{0}$
$m_2 = 2.5\times10^{0}$
$c_2 = 1.0\times10^{0}$
De-scaling of output parameter
$m_1 = 1.001\times10^{0}$
$c_1 = -6.14\times10^{-1}$

Table 10
Artificial neural network parameters for direct estimation of nondimensional heat transfer coefficient, B in nonlinear problem from slope, s at location $X = 0.2$

i	j	bias	w_{ij}	j	k	bias	w_{jk}
1	1	-6.37×10^{-1}	-1.029×10^{0}	1	1	1.31×10^{-1}	-8.96×10^{-1}
1	2	-3.63×10^{-1}	-3.71×10^{-1}				-3.61×10^{-1}

$At\ X = 0.2$
B, $0.01 \leqslant B \leqslant 50.0$
s, $0.045 \leqslant s \leqslant 0.981$
Input and output parameters
$U_1 = \text{atan}(s)$
$S_1 = \text{atan}(B)$

Scaling of input parameters	De-scaling of output parameter
$m_1 = 2.738 \times 10^{0}$	$m_1 = 1.284 \times 10^{0}$
$c_1 = -1.123 \times 10^{0}$	$c_1 = 7.804 \times 10^{-1}$

References

[1] S. Chantasiriwan, Inverse determination of steady state heat transfer coefficient, International Communication in Heat and Mass Transfer 27 (2000) 1155–1164.

[2] J.V. Beck, B. Blackwell, C.R.St. Clair Jr., Inverse Heat Conduction, John-Wiley-Interscience, New York, 1985.

[3] J.V. Beck, K.J. Arnold, Parameter Estimation in Engineering and Science, John Wiley and Sons, New York, 1977.

[4] O.M. Alifanov, Inverse Heat Transfer Problems, Springer Verlag, Berlin, Germany, 1994.

[5] M.N. Ozisik, H. Orlande, Inverse Heat Transfer, Fundamentals and Applications, Taylor and Francis, New York, NY, 2000.

[6] V. Dumek, M. Druckmuller, Raudensk, K.A. Woodbury, Novel Approaches to the ICHP: Neural Networks and Expert Systems, Inverse Problems in Engineering: Theory and Practice, in: Proceedings of the First International Conference on Inverse Problems in Engineering, ASME no. I00357, 1993, p. 275–282.

[7] K. Jambunathan, S. Hartle, S Ashforth-Frost, V.N. Fontama, Evaluating convective heat transfer coefficients using neural networks, International Journal of Heat and Mass Transfer 39 (1996) 2329–2332.

[8] G. Porru, C. Aragonese, R. Baratti, A. Servida, Monitoring of a CO oxidation reactor through a grey model-based EKF observer, Chemical Engineering Sciences 55 (2000) 331–338.

[9] S.S. Sablani, A neural network approach for non-iterative calculation of heat transfer coefficient in fluid-particle systems, Chemical Engineering and Processing 40 (2001) 363–369.

[10] A. Pacheco-Vega, M. Sen, K.T. Yang, R.L. McClain, Neural network analysis of fin-tube refrigeration heat exchanger with limited experimental data, International Journal of Heat and Mass Transfer 44 (2001) 763–770.

[11] A. Pacheco-Vega, G. Diaz, M. Sen, K.T. Yang, R.L. McClain, Heat rate predictions in humid air-water heat exchangers using correlations and neural networks, ASME Journal of Heat Transfer 123 (2001) 348–354.

[12] G. Diaz, M. Sen, M.K.T. Yang, R.L. McClain, Dynamic prediction and control of heat exchangers using artificial neural networks, International Journal of Heat and Mass Transfer 44 (2001) 1671–1679.

[13] S.S. Sablani, W.H. Shayya, A. Kacimov, Explicit calculation of the friction factor in pipeline flow of Bingham plastic fluids: a neural network approach, Chemical Engineering and Sciences 58 (2003) 99–106.

[14] B. Huang, A.S. Mujumdar, Use of neural network to predict industrial dryer performance, Drying Technology-An International Journal 11 (1993) 525–541.

[15] H.Y. Fan, W.Z. Lu, G. Xi, S.J. Wang, An improved neural network based calibration method for aerodynamic pressure probes, ASME Journal of Fluids Engineering 125 (2003) 113–120.

[16] H.S. Carslaw, J.C. Jaeger, Conduction of Heat in Solids, Oxford University Press, London, 1959.

[17] S. Wolfram, Mathematica. A System for Doing Mathematics by Computer, Addison-Wesley, Redwood City, 1991.

[18] Yu.I. Malov, L.K. Martinson, K.B. Pavlov, Solution of some mixed boundary-value problems of heat conduction, Ingenerno-Fizicheskij Zhurnal 28 (1974) 336–340 (in Russian).

[19] D.H.Y. Yen, J.V. Beck, R.L. McMaster, D.E. Amos, Solution of an initial-boundary value problem for heat conduction in a parallelepiped by time partitioning, International Journal of Heat and Mass Transfer 45 (2002) 4267–4279.

[20] A.A. Samarskii, V.A. Galaktionov, S.P. Kurdyumov, A.P. Mikhailov, Blow-up in Quasilinear Parabolic Equations, Nauka, Moscow, 1987, in Russian (Engl. transl.: Walter de Gruyter, Berlin, 1995).

[21] G.I. Barenblatt, V.M. Entov, V.M. Ryzhik, Theory of Fluid Flows through Natural Rocks, Kluwer, Dordrecht, 1990.

[22] K. Hornik, M. Stinchombe, H. White, Multilayer feed forward network are universal approximators, Neural Networsk 2 (1989) 359–366.

[23] G. Scalabrin, L. Piazza, Analysis of forced convection heat transfer to supercritical carbon dioxide inside tubes using neural networks, International Journal of Heat and Mass Transfer 46 (2003) 1139–1154.

[24] C. Le Niliot, F. Lefevre, A parameter estimation approach to solve the inverse problem of point heat sources

identification, International Journal of Heat and Mass Transfer 47 (2004) 827–841.

[25] S. Sreekanth, H.S. Ramaswamy, S.S. Sablani, S.O. Prasher, A neural network approach for inverse heat transfer problems, American Society of Mechanical Engineers National Heat Transfer Conference Baltimore MD 1997, August 10–12.

[26] M.R. Islam, S.S. Sablani, A.S. Mujumdar, An artificial neural network model for prediction of drying rates, Drying Technology-An International Journal 21 (2003) 1871–1888.

[27] G.B. Awuah, H.S. Ramaswamy, B.K. Simpson, Comparison of two methods for evaluating fluid to particle surface heat transfer coefficients, Food Research International 28 (1995) 261–271.